Materials for Renewable and Sustainable Energy (2018) 7:13
https://doi.org/10.1007/s40243-018-0119-7

ORIGINAL PAPER

Fabrication of titanium dioxide (TiO_2) and mercury sulfide (HgS) heterojunction for photoelectrochemical study

Rahul A. Wagh[1,2] · Anil N. Kulkarni[2] · Prashant K. Baviskar[3] · Habib M. Pathan[3] · Rajendra S. Patil[1]

Received: 22 November 2017 / Accepted: 24 April 2018 / Published online: 15 May 2018

Abstract
This work reports a chemical solution sensitization of HgS nanocrystals on mesoporous TiO_2 films for different deposition times. The adsorption of the precursor ions and the surface growth of the crystal were found to be affected during the temporal deposition of the HgS over spin-coated TiO_2 films. The synthesized electrodes were characterized by structural, morphological, wettability, optical, photovoltaic, and electrochemical performances. The results designate the qualitative confirmation of the TiO_2/HgS heterojunction formation, and the combination is explored for the photovoltaic application, which is first of its kind.

Keywords Spin coating · Mercury sulfide · Titanium dioxide · Heterojunction · Optical properties

Introduction

Several strategies have been explored to extend the optical absorption of TiO_2 into the visible light region including doping of metal or nonmetal ions, dye sensitization, surface modification, and coupling with narrow bandgap semiconductors [1–8]. Among these, a remarkable enhancement in the photoelectrochemical (PEC) performance of TiO_2 under light has been obtained by coupling low bandgap semiconductors such as CdS [4], CdSe [5], Ag_2S [6], Sb_2S_3 [7], and Bi_2S_3 [8]. However, to date, all such heterojunction-based solar cells do not meet the theoretical value for light-harvesting efficiency reported in the literature [9]. This is because of the one of the limits that a large amount of the incident solar radiation is not absorbed by the solar cells. This deterrent has resulted in search for the different light-harvesting sensitizers to enhance the light absorption capacity in the visible and near infra-red (IR) region of the solar spectrum.

Mercury sulfide (HgS), a group II–VI compound with cubic phase [9] having bulk bandgap about 0.5 eV [10], which is tunable in the range of about 1.9–2.6 eV [9], suggests it an alternative candidate to above discussed sensitizers. The literature also reveals that the conduction band position of HgS and TiO_2 w.r.t. vacuum is favorable [11], which proposes TiO_2/HgS heterojunction configuration, a potential candidate for photovoltaic applications. However, the literature survey indicates that the photovoltaic studies of HgS sensitized TiO_2 photoelectrode are not reported earlier. And so, it is important to explore HgS as a sensitizer for TiO_2 photoelectrode toward photovoltaic application. Thus, in the present work, we demonstrate the temporal chemical solution deposition of HgS nanocrystals over spin-coated titanium dioxide for photovoltaic application.

Experimental details

Materials

TiO_2 (P-25, Degussa, Germany), acetyl acetone, *p*-hydroxybenzoic acid, ethanol, mercury chloride, and sodium thiosulfate were analytical reagent (AR) grade and used without further purification. Fluorine-doped tin oxide (FTO) is used as substrate for deposition of TiO_2.

✉ Rahul A. Wagh
rahulawagh26@gmail.com

[1] Department of Physics, P. S. G. V. P. Mandal's Arts, Commerce and Science College, Shahada Dist., Nandurbar, Maharashtra, India

[2] Department of Physics, School of Science, Sandip University, Nashik, Maharashtra, India

[3] Advanced Physics Laboratory, Department of Physics, Savitribai Phule Pune University, Pune, Maharashtra, India

Synthesis of TiO_2 film by spin-coating technique

In the present work, TiO_2 photoelectrodes were prepared onto FTO substrates using spin-coating technique at room temperature. Prior to deposition, FTO substrates were washed with detergent and then cleaned with double-distilled water (DDW). Again, the substrates were rinsed ultrasonically with DDW before deposition of thin films. Initially, TiO_2 nanoparticles (P-25, Degussa, Germany), precursor for TiO_2, ethanol, and acetyl acetone, solvents, and catalyst were used for the preparation of gel of TiO_2 using the sonication method. First, 2 g of TiO_2 powder (Degussa P-25), 8.5 ml of ethanol, and 1.5 ml acetyl acetone are added together in a beaker and stirred together for 30 min. Second, 1 g *p*-hydroxybenzoic acid and catalyst were added to the above mixture and allowed for continuous stirring for next 8 h at room temperature until a uniform mixture is formed. Third, the obtained homogeneous mixture was sonicated for 30 min after transferring them into a clean 10-ml beaker with the frequency of 20 kHz using ultrasonication bath.

For the preparation of TiO_2 samples, 1 ml of TiO_2 gel was introduced over the cleaned substrate and then rotated for 2 min. Furthermore, the coated samples were annealed at 400 °C for 45 min.

Deposition of HgS over spin-coated TiO_2

The deposition process of HgS involves mercury chloride ($HgCl_2$) and sodium thiosulphate ($Na_2S_2O_3$) as a precursor of mercury ions (Hg^{2+}) and sulfide ions (S^{2-}), respectively. First, for the deposition of HgS films, aqueous solution of $HgCl_2$ (0.04 M) and $Na_2S_2O_3$ (0.08 M) in 10 ml of DDW was prepared in two different beakers. Initially, the beaker containing $HgCl_2$, source of Hg^{2+}, is kept on constant stirring at room temperature, and $Na_2S_2O_3$, source of S^{2-}, is added slowly in the first bath. The formed mixture is stirred well to dissolve the formed precipitate, which leads to the homogeneous solution. Now, the deposition process was considered to be based on slow release of Hg^{2+} and S^{2-} ions in the solution which then condense as ion by ion or cluster by cluster mechanism on the surface of substrate, as a result of heterogeneous nucleation reported earlier [8].

Now, spin-coated FTO/TiO_2 samples were introduced vertically into the bath of HgS, for the purpose of the chemical solution deposition of HgS at 70 °C for three different deposition times, namely 30, 45, and 60 min. The samples were nomenclated as A, B, and C, respectively. The porous film of TiO_2 was observed to be coated with the enhanced brownish shade of the photoanodes with the increase in the deposition time. This might be due to the enhanced level of deposition of nanocrystalline HgS onto the bare photoanodes of TiO_2 with increased sensitization time.

Thereafter, to enhance the crystallinity of HgS crystals, samples A–C were annealed for 30 min at 200 °C.

Cell assembly

For the measurement of photoelectrochemical cell (PEC) performance, we have used the aqueous solution of polysulfide electrolyte which was prepared using the 1 M of sodium sulfide (Na_2S), 1 M of sulfur powder, and 1 M of sodium hydroxide (NaOH). For cell assembly, the carbon suit of FTO was used as a counter electrode. All three samples A–C and counter electrode were clamped together into a sandwich-type configuration with droplet of polysulfide electrolyte injected in between them, for the fabrication of solar cells.

Characterization of HgS, TiO_2, and TiO_2/HgS thin films

The structural analysis was carried out using X-ray diffractometry by means of an automated Bruker D8 advance X-ray diffractometer. Optical absorption study was carried out using a JASCO UV–Vis spectrophotometer (V-630) at room temperature. A scanning electron microscope (SEM) with an energy-dispersive spectrometer (EDS) attachment [S-4800 Type-II (Hitachi High Technology Corporation Tokyo, Japan)] was used to study morphological and elemental analysis of the samples. Contact angle measurement (CAM) has been measure with the help of lab made facility using DSC-HX7V cyber shot camera with 16.2 Mega pixels sensor and 10x optical zoom. The cell performance was measured by a semiconductor characterization unit (Keithley 2420 source meter) under illumination of 85 mW/cm^2. Electrochemical impedance spectroscopy (EIS) was studied by potentiostat/galvanostat (IVIUM Vertex model).

Results and discussion

Structural analysis

The XRD patterns of the HgS and TiO_2 are shown in Fig. 1a, b, which reveals the hexagonal phase for the deposited HgS crystals (JCPDS data file: 421408) and anatase phase with tetragonal structure for the spin-coated TiO_2 films (JCPDS data file: 84-1285).

However, the XRD pattern shown in Fig. 1c comprises combinations of two sets of patterns: one of them is assigned to TiO_2 (JCPDS data file: 84-1285) and other originates from the HgS (JCPDS data file: 421408). This confirms the formation of heterojunction between TiO_2 and HgS crystals deposited using chemical solution technique.

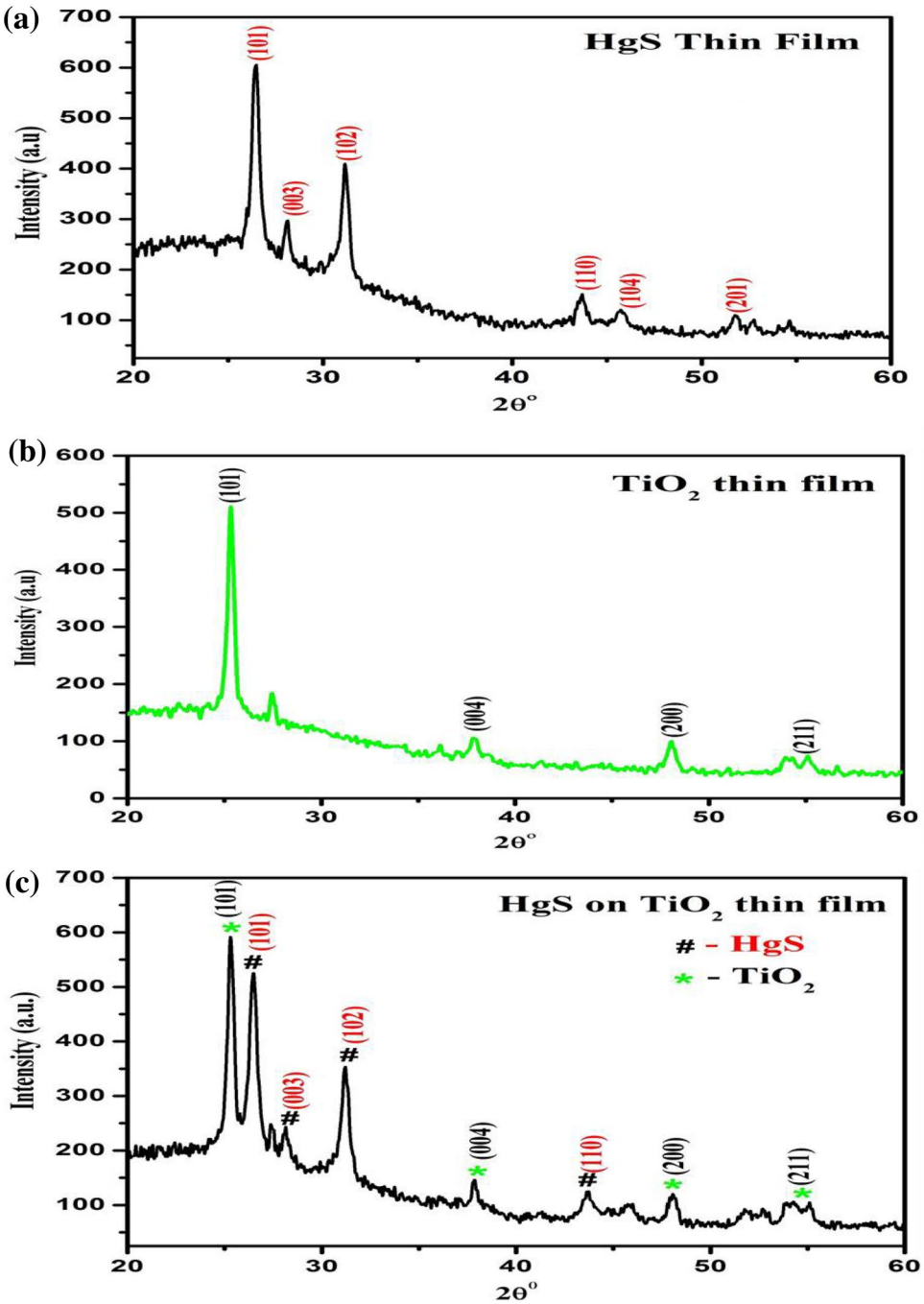

Fig. 1 2θ versus intensity plot of **a** HgS, **b** TiO_2, and **c** HgS sensitized TiO_2 photoanodes

Morphological analysis and contact angle measurement of HgS, TiO_2, and TiO_2/HgS films

Figure 2a–c shows the surface morphology analysis of HgS, TiO_2, and TiO_2/HgS films, respectively. Figure 2a shows that the substrate is uniformly covered with HgS, having spherical morphology. The flake-like network of TiO_2 crystals is observed from Fig. 2b. However, from Fig. 2c, it is observed that in case of TiO_2/HgS sample, surface is covered with enhanced granular structure. This depicts the coating of HgS nanoparticles over the entire surface of porous TiO_2 films.

Besides as shown in Fig. 2a–c, the wettability of the samples studied using CAM for TiO_2/HgS film is 31°, which is smaller than the bare TiO_2 film (52°). The improved wettability of TiO_2/HgS after sensitization is helpful for the diffusion of electrolyte and charge transport at the interfaces between photoanode and electrolyte [12].

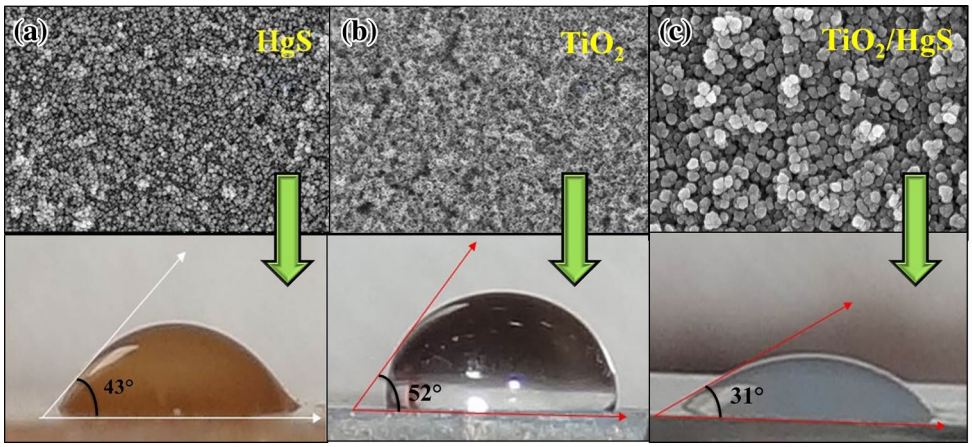

Fig. 2 Scanning electron micrographs and contact angle measurement of **a** HgS, **b** TiO_2, and **c** TiO_2/HgS photoanodes

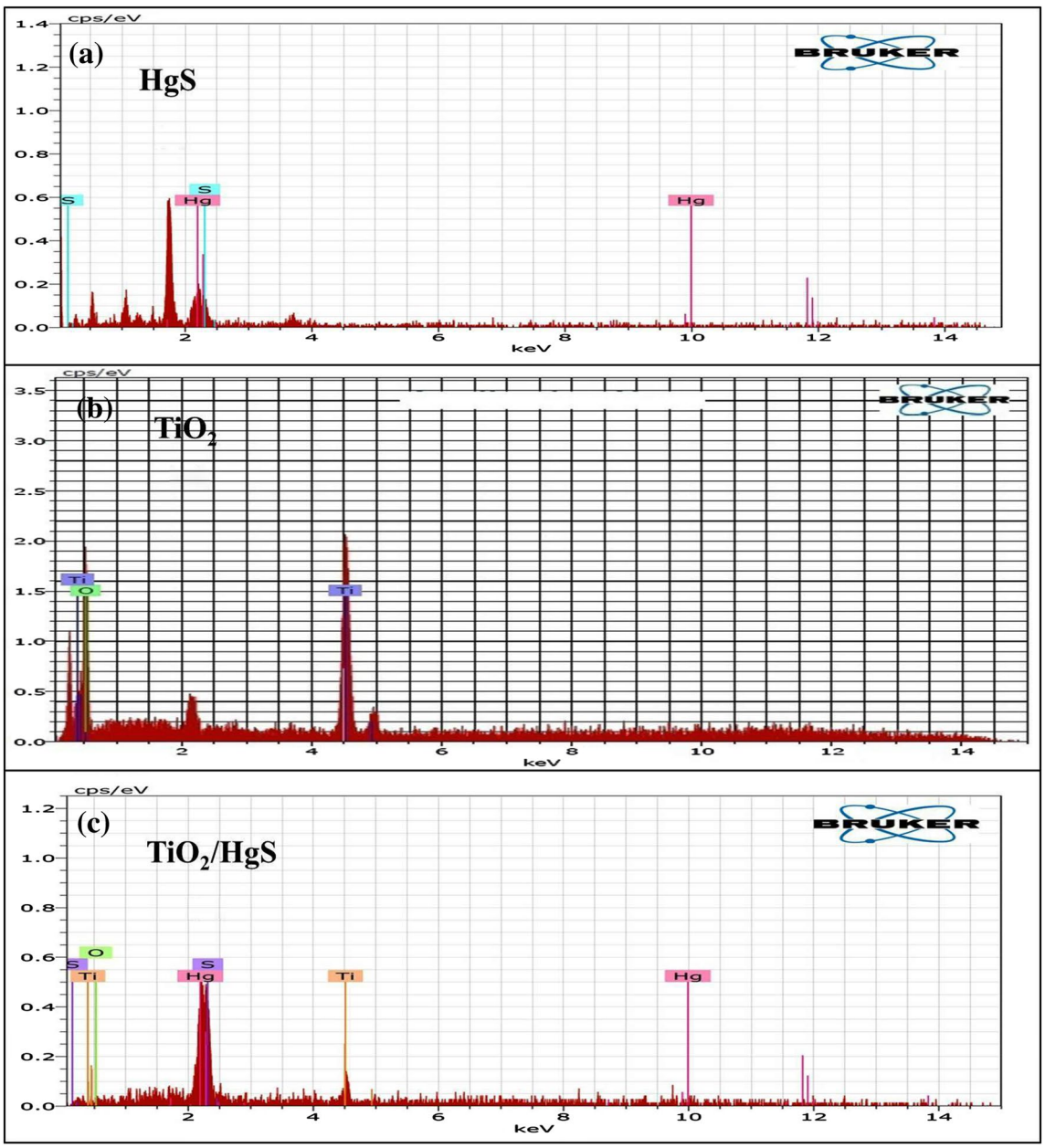

Fig. 3 EDXS spectrum of HgS, TiO_2, and HgS sensitized TiO_2 photoelectrodes

Elemental analysis

Figure 3a–c shows a comparative elemental analysis of HgS, TiO_2, and TiO_2/HgS photoelectrodes, respectively. The presence of emission lines of 'Ti', 'Hg', 'S', and 'O' in the energy-dispersive X-ray spectroscopy (EDXS) spectra for TiO_2/HgS film gives qualitative confirmation of the chemical bath deposition (CBD) of the HgS over the TiO_2 film, which matches with TiO_2/HgS heterojunction formation analysis discussed above in XRD analysis.

Optical properties

Figure 4 displays the UV–visible spectra curves of the TiO_2 films loaded with HgS nanocrystals for different deposition times. It is clear that both absorbance and absorption range of the TiO_2 films are proportional to the number density of HgS nanocrystals. The observed shift of the absorbance edge toward the red edge suggests that the TiO_2 film after HgS deposition may cover the entire visible and near IR region of the solar spectrum. Such enhanced absorption in the visible region, which causes the blue shift in the energy bandgap for TiO_2/HgS films (Fig. 4b), indicates the lowering of the conduction band of the TiO_2 [13]. This may provide a driving force in the charge separation process at the interface of HgS and TiO_2.

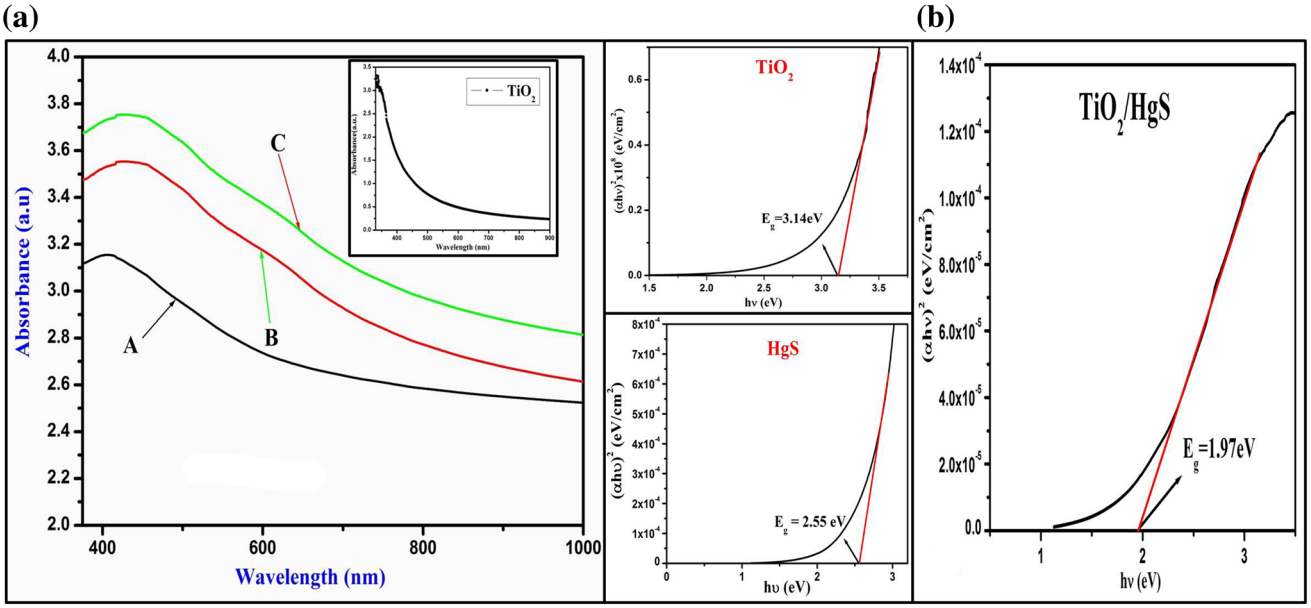

Fig. 4 **a** Wavelength-dependent absorption spectra of bare TiO_2 and TiO_2/HgS films. **b** Optical energy bandgap of bare TiO_2, HgS, and TiO_2/HgS film

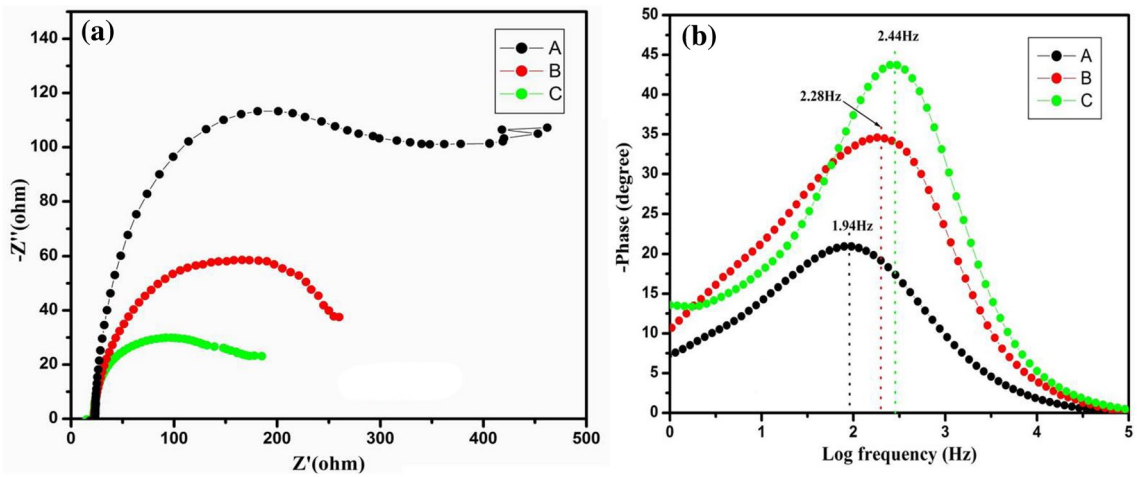

Fig. 5 **a** Nyquist plot for cells A, B, and C. **b** Bode plot for cells A, B, and C

Table 1 Electron lifetime for the different electrode systems

Cell assembly	Deposition time (min)	Life time τ (ms)
A	30	12
B	45	6.2
C	60	4.65

Electrochemical impedance spectroscopy

Figure 5a shows electrochemical impendence spectra (EIS) curves for the cells A–C under the dark condition. It comprises two semicircles: first gives the charge transfer resistance at the counter electrode/polysulfide electrolyte interface, and the second circle represents charge transfer and transport at the TiO_2/HgS/polysulfide interface.

In the present work, EIS result shows the enlarged radius of the second semicircle in the Nyquist plot for cell A. This is probably due to the very less number and size of HgS nanocrystals, in case of sample A. However, for increased deposition time up to 45 min, there is a decrease in the radius of the semicircle in the Nyquist plot for cell B. This may be because of the enhancement in the size and number of HgS nanocrystals over TiO_2, which is in agreement with optical absorption study discussed above. Further, as shown in Fig. 5a, in case of cell C, there is a sudden decrease in the radius of the semicircle in the Nyquist plot. Such a result may be attributed to the aggregation of HgS, leading to clogging of the TiO_2 pores. The apparent red shift in the optical absorption spectra for sample C supports such an aggregation.

Figure 5b shows the Bode plots of the solar cells A–C. The curve peak of the spectrum can be used to determine the electron lifetime according to the equation $\tau = 1/(2\pi f)$ [14], where τ = electron lifetime and f = maximum frequencies from Bode plot, and is presented in Table 1.

Thus, according to the results of the optical absorption, electron transfer, and life time, the optimal coating of HgS may have sped up the charge transport and results in the enhanced photocurrent for cell B. This suggests 45 min as appropriate sensitization time for HgS nanocrystals over TiO_2 in the present study.

PEC performance

Figure 6 shows current density–voltage (J–V) characteristics of HgS sensitized TiO_2 solar cells. The device B shows a better performance than the devices A and C, respectively. The obtained photovoltaic parameters are tabulated in Table 2.

As discussed earlier, with increase of sensitization time, the optical absorption spectra as shown in Fig. 4a clearly show an enhanced loading of the sensitizer into the photoelectrodes, which is evident from the improved optical absorption in the visible region. However, the enlarged arc of Nyquist plot for cell A suggests the deposition of less number of HgS nanocrystals for the deposition time of 30 min. Thus, instead of maximum life time, cell A gives

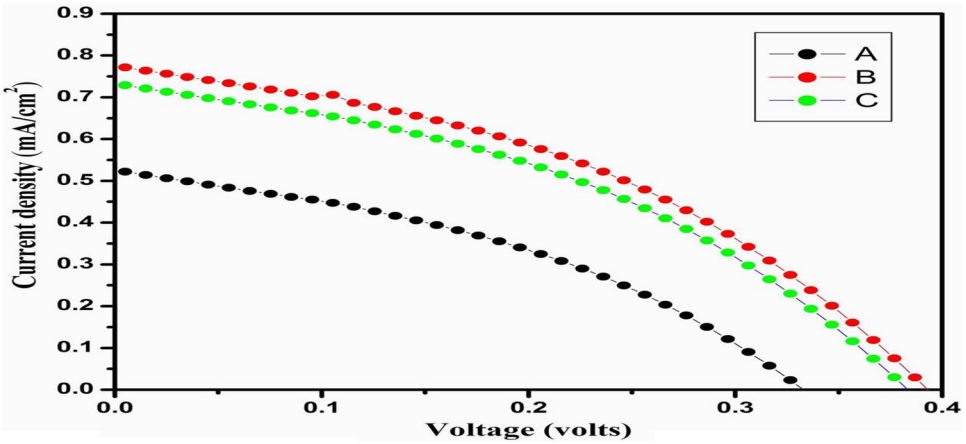

Fig. 6 Photocurrent density (J_{sc}) versus photovoltage (V_{oc}) characteristic curves for cells A, B and C

Table 2 Solar cell parameters for samples A, B, and C

Cell assembly	Deposition time	J_{sc} (mA/cm^2)	V_{oc} (mV)	FF (%)	Efficiency (%)
FTO/TiO_2/HgS/polysulphide/carbon suit-FTO	A (30 min)	0.53	330	17	0.24
	B (45 min)	0.77	393	22	0.39
	C (60 min)	0.72	381	20	0.31

rise to less current density J_{sc} and open-circuit voltage V_{oc} under illumination, as tabulated in Table 2.

Nevertheless, in case of sample B, the stretched optical absorbance in the far visible region compared to sample A reveals increased size and number of HgS nanocrystals for the deposition time of 45 min. Such an enhanced absorption of light in the visible region leads to the generation of increased number density of excitons at the electrode–electrolyte interface. This gives rise to the enhanced photocurrent J and hence J_{sc} in case of cell B, even if the lifetime is observed to be decreased from 12 to 6.2 ms.

Conversely, the observed declined performance for cell C may be attributed to the aggregation of HgS nanocrystals, resulting in the decrease of the access of electrolyte into the pores of photoanode. This may have increased the recombination probability in the film, which may be confirmed from the minimized life time in case of cell C.

Conclusion

We have demonstrated the successful chemical bath deposition of hexagonal HgS crystals over the anatase TiO_2 photoanode for solar cell application, which is first of its kind. The process of the HgS deposition on the surface of the TiO_2 film was heterogeneous nucleation, which was visibly affected by the deposition time. The appropriate deposition time was determined as 45 min for the TiO_2/HgS heterojunction using electron transfer and lifetime measurements through EIS. For the deposition time beyond 45 min, i.e., 60 min, the photovoltaic properties of TiO_2/HgS-based cell started dropping due to the increased surface-charge recombination.

Acknowledgement The author sincerely acknowledges the University Institute of Chemical Technology (UICT), North Maharashtra University, Jalgaon, and Tata Institute of Fundamental Research (TIFR), Mumbai, for providing the characterization facilities. RAW and ANK are also thankful to the Management and Hon'ble Vice-Chancellor, Sandip University, Nashik, for providing laboratory facility.

References

1. Daghrir, R., Drogui, P., Robert, D.: Modified TiO_2 for environmental photocatalytic applications: a review. Ind. Eng. Chem. Res. **52**, 3581–3599 (2013)
2. Sato, T., Yamamoto, Y., Fujishiro, Y., Uchida, S.: Intercalation of iron oxide in layered $H_2Ti_4O_9$ and $H_4Nb_6O_{17}$: visible-light induced photocatalytic properties. J. Chem. Soc. **92**, 5089–5092 (1996)
3. Choy, J.H., Lee, H.C., Jung, H., Hwang, S.J.: A novel synthetic route to TiO_2-pillared layered titanate with enhanced photocatalytic activity. J. Mater. Chem. **11**, 2232–2234 (2001)
4. Yang, H., Jin, Z., Hu, H., Lu, G., Bi, Y.: Fabrication and behaviors of CdS on Bi_2MoO_6 thin film photoanodes. RSC Adv. **7**, 10774–10781 (2017)
5. Zhaoa, F., Tanga, G., Zhang, J., Linb, Y.: Improved performance of CdSe quantum dot-sensitized TiO_2 thin film by surface treatment with $TiCl_4$. Electrochim. Acta **62**, 396–401 (2012)
6. Wagh, R.A., Salunke, D.B., Gosavi, S.R., Patil, R.S.: Effect of uniform decoration of Ag_2S nanoparticles on physical properties of granular TiO_2 thin films synthesized by using spin coating technique. J. Nano-Electron. Phy. **8**, 04080-1-04080-5 (2016)
7. Kulkarni, A.N., Arote, S.A., Pathan, H.M., Patil, R.S.: Room temperature synthesis of crystalline Sb_2S_3 for SnO_2 photoanode-based solar cell application. Bull. Mater. Sci. **38**, 493–498 (2015)
8. Kulkarni, A.N., RajendraPrasad, M.B., Pathan, H.M., Patil, R.S.: TiO_2 photoanode sensitized with nanocrystalline Bi_2S_3: the effect of sensitization time and annealing on its photovoltaic performance. Appl. Nanosci. **6**(4), 567–574 (2016)
9. Chaitanya, K., Ju, X.H., Heron, B.M.: Theoretical study on the light harvesting efficiency of zinc porphyrin sensitizers for DSSCs. RSC Adv. **4**, 26621–26634 (2014)
10. Chakraborty, I., Mitra, D., Moulik, S.P.: Spectroscopic studies on nanodispersions of CdS, HgS, their core-shells and composites prepared in micellar medium. J. Nanopart. Res. **7**, 227–236 (2005)
11. Yong, X., Martin, A.A.: Schoonen.: the absolute energy positions of conduction and valence bands of selected semiconducting minerals. Am. Mineral. **85**, 543–556 (2000)
12. Kulkarni, A.N., Arote, S.A., Pathan, H.M., Naushad, M., Patil, R.S.: Bismuth sulphide sensitized tin oxide photoelectrode for solar cell application. Indian J. Phys. **90**, 887–893 (2016)
13. Tachibana, Y., Moser, J.E., Gratzel, M., Klug, D.R., Durran, J.R.: Subpico second interfacial charge separation in dye-sensitized nanocrystalline titanium dioxide films. J. Phys. Chem. B **100**, 20056–20062 (1996)
14. Majumder, S., Baviskar, P.K., Sankapal, B.R.: Light-induced electrochemical performance of 3D-CdS nanonetwork: effect of annealing. Electrochim. Acta **222**, 100–107 (2016)